A Microfluidic Mixer Utilizing Electrokinetic Relay Switching and Asymmetric Flow Geometries

Yiou Wang

Jiang Zhe

Department of Mechanical Engineering,
The University of Akron,
Akron, OH 44325

Prashanta Dutta
School of Mechanical and Materials Engineering,
Washington State University,
Pullman, WA 99164-2920
e-mail: dutta@mail.wsu.edu

Benjamin T. Chung
Department of Mechanical Engineering,
The University of Akron,
Akron, OH 44325

Performances of a hybrid electrokinetic-passive micromixer are predicted numerically. An h/p-type spectral element method is used to simulate the mixing behavior in microdevices. The numerical algorithm employs modal spectral expansion in quadrilateral and unstructured triangular meshes and provides high-order numerical accuracy. A second-order accurate, stiffly stable integration scheme is used for temporal integration. In the numerical technique, the electric double layer is not resolved to avoid expensive computation, rather a slip velocity is assigned at the channel surface based on the electric field and the electroosmotic mobility. The presented hybrid mixing scheme takes advantages of mixing enhancements induced by asymmetric flow geometries and electrokinetic relay actuation. Effects of relay frequency, applied electric potential, channel width, and channel geometry on micromixing have been conducted. Numerical results show that electrokinetic relay at an appropriate frequency causes effective mixing. Moreover, asymmetric flow geometries and narrow channel width are critical for ultraeffective mixing. The proposed hybrid mixing scheme not only provides excellent mixing within very short time, but also can easily be integrated with microdevices for "lab-on-a-chip" applications because there is no need of any external mechanical pumps. [DOI: 10.1115/1.2436578]

Keywords: electrokinetic flow, hybrid mixing, microfluidic, zeta potential

1 Introduction

Mixing of liquid samples is an important task in microfluidic-based biological and chemical systems, such as "lab-on-a-chip" or micro-total-analysis-systems (μTAS) applications. Rapid mixing permits quick processing and analysis of samples and, hence, allows a high throughput system. However, fast mixing in microchannels has been a challenging problem. Because of the nature of laminar flow in the microscale, mixing is mainly dominated by diffusion. In the absence of any turbulence, it is difficult to improve the mixing simply through diffusion. In particular, for large molecules, such as DNA and proteins, the diffusion coefficients are on the order of 10^{-10} m^2/S or less. Hence, the resulting mixing time and the mixing length can both be prohibitively long and impractical. A highly efficient micromixer that permits fast mixing is greatly expected to benefit a number of critical applications, such as DNA hybridation, cytometric analysis, and immunoassays.

Existing micromixers fall into two categories: active mixers and passive mixers. Passive mixers have been studied extensively because of the advantages of low cost, ease of fabrication, and no need for additional power input. Passive mixers have no moving parts and achieve mixing by virtue of their structure or topology alone. Using passive structures, the fluids are forced to change directions, split, or reunify to increase the contact areas of substreams [1–4]. As the microchannel dimensions are scaled down to smaller values, larger flow impedance will be generated that requires higher pump power. Thus, most passive mixers reported thus far only show relatively high mixing efficiency at a low flow rate. Recently, a rotation mechanism has been introduced to increase the contact area by utilizing three-dimensional (3D) serpentine microchannel and bias-relief structures [5,6]. In spite of high mixing efficiency at high flow rates, the complex 3D structures are hard to fabricate and create large flow impedances.

Active mixers can produce excellent mixing by using external energy. A variety of active chaotic mixing schemes has been applied to microfluidic devices to enhance the micromixing efficiency. These schemes include electrokinetic mixing [7–9], ultrasonic excitation [10], magnetic stirring [11], thermal bubble mixing [12], magnetic beads excitation [13,14], dielectrophoretic mixing [15], bubble acoustic agitation [16], shear superposition micromixer [17], etc. Among them, electrokinetic mixing is a favorable mixing scheme for ease of manufacturability and simplicity. Another advantage is that electrokinetic mixing scheme can be easily integrated into the microfluidic chips. Furthermore, there is no penalty of dramatic pressure drop with electrokinetic driven flow. Recently, He et al. [18] reported a micromixer based on flow splitting and a lateral transport mechanism under electroosmotic flow at a low flow rate. Johnson et al. [19] presented a T-microchannel with ablated walls for improving mixing efficiency over a broad range of electroosmotic flow rates.

Although passive mixing and electrokinetic relay mixing are efficient mixing schemes, if one mixing mechanism is used individually, it cannot meet the requirements in some biochemical analysis for μTAS applications because the mixing times are in the order of seconds, especially at large flow rates. In this paper, a numerical study is presented for a hybrid rapid micromixer. The proposed hybrid micromixer takes advantages of both mixing enhancements induced by asymmetric serpentine structures and the electrokinetic relay actuation. In order to obtain the high mixing performance, the effects of microchannel geometry, electrokinetic relay frequency, and electric field strength on mixing performance are investigated systematically.

The rest of the paper is organized as follows. In Sec. 2, the micromixer design is introduced. In Sec. 3, the mathematical model for the electrokinetic relay mixing is presented along with underlying assumptions and approximations. Next, the numerical algorithm used to compute the electric field, velocity field, and concentration in the microfluidic mixer is discussed. In Sec. 5,

Contributed by the Fluids Engineering Division of ASME for publication in the JOURNAL OF FLUIDS ENGINEERING. Manuscript received February 3, 2006; final manuscript received June 29, 2006. Review conducted by Ali Beskok. Paper presented at the 2005 ASME International Mechanical Engineering Congress (IMECE2005), Orlando, Florida, November 5–11, 2005.

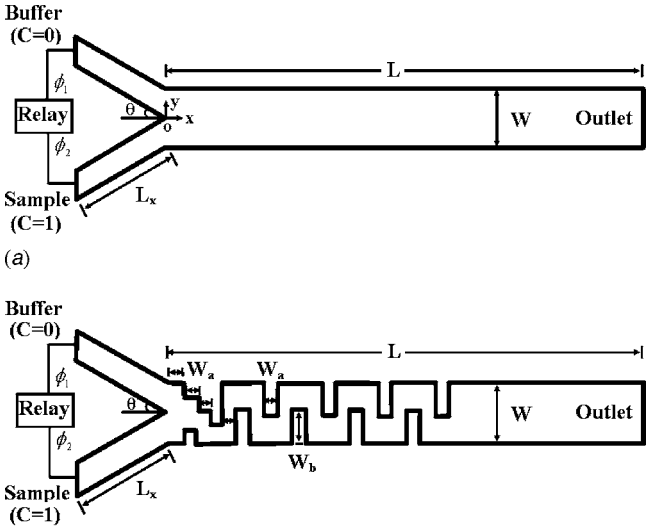

Fig. 1 Schematic diagram of (*a*) electrokinetic relay micromixer and (*b*) hybrid (electrokinetic asymmetric structure) micromixer

simulation results are provided for electrokinetic relay mixer and hybrid mixer. Finally, a summary and conclusions of this numerical work are presented.

2 Micromixer Design

Figure 1(*a*) shows the schematic view of a Y-form electrokinetic micromixer considered in this study. Two different fluids are periodically pumped into the mixing chamber through two branches of Y-channel. Inlet 1 brings buffer solution of scalar concentration $C=0$, and inlet 2 feeds sample solution of scalar concentration $C=1$. In this study, an electrokinetic pumping mechanism is used to drive the fluid from inlet reservoirs to outlet through the mixing chamber. In order to obtain electrokinetic relay effects, the externally applied electric potentials at inlets 1 and 2 are set as

$$\phi_1 = \phi_s + m(t)\phi_a \tag{1}$$

$$\phi_2 = \phi_s + [1 - m(t)]\phi_a \tag{2}$$

where ϕ_s and ϕ_a are the steady and alternating parts of the externally applied electric potential, respectively. The time-dependent parameter $m(t)$ is given as

$$m(t) = 0, \quad \text{if} \quad \sin(\pi f t) > 0 \tag{3}$$

$$m(t) = 1, \quad \text{if} \quad \sin(\pi f t) \leq 0 \tag{4}$$

In this paper, we set $L_x=200$ μm, $L=1000$ μm, and $\theta=30$ deg. The channel width (W), applied electric potentials (ϕ_s and ϕ_a), and relay frequency (f) are varied from case to case. The width of each inlet channel is one-half of the width of mixing channel. To further intensify the mixing, asymmetric serpentine structures are placed into the mixing channel, as shown in Fig. 1(*b*).

3 Mathematical Model

Electroosmotic flow is the bulk motion of an electrolyte solution under the action of an electric field. When an electrolyte comes in contact with a channel (dielectric) surface, the surface generally acquires net surface charges due to ionization, ion adsorption, or ion absorption. These surface charges influence the distribution of counterions close to the surface, and form an electric double layer (EDL) adjoining to the surface. The extent of EDL depends on the ion concentration in the electrolytes and is normally characterized by the Debye layer thickness (λ). For example, ion concentration of 1 mM and 100 mM corresponds to Debye length thickness of 10 nm and 1 nm, respectively. If an external electric field, $\vec{E}=-\nabla\phi$, is applied along the channel surface by setting electric potential (ϕ) at end reservoirs, there will be net movement of electrolyte due to the formation of an electrokinetic body force. The governing equations for ionized incompressible flow with electrokinetic body forces are given by the continuity and Navier-Stokes equations [20]

$$\frac{\partial u}{\partial x} + \frac{\partial v}{\partial y} = 0 \tag{5}$$

$$\rho_f\left(\frac{\partial \mathrm{u}}{\partial \mathrm{t}} + u\frac{\partial u}{\partial x} + v\frac{\partial u}{\partial y}\right) = -\frac{\partial P}{\partial x} + \mu\left(\frac{\partial^2 u}{\partial x^2} + \frac{\partial^2 u}{\partial y^2}\right) + \rho_e E_x \tag{6}$$

$$\rho_f\left(\frac{\partial v}{\partial t} + u\frac{\partial v}{\partial x} + v\frac{\partial v}{\partial y}\right) = -\frac{\partial P}{\partial y} + \mu\left(\frac{\partial^2 v}{\partial x^2} + \frac{\partial^2 v}{\partial y^2}\right) + \rho_e E_y \tag{7}$$

where u is the streamwise velocity, v is the cross-stream velocity, ρ_f and ρ_e are the fluid density and electric charge density, respectively, t is the time, P is the pressure, and μ is the viscosity. The externally applied electric potential (ϕ) is governed by the charge conservation equation

$$\frac{\partial}{\partial x}\left(\sigma\frac{\partial \phi}{\partial x}\right) + \frac{\partial}{\partial y}\left(\sigma\frac{\partial \phi}{\partial y}\right) = 0 \tag{8}$$

where σ is the electrical conductivity of fluid. The electrokinetic potential distribution (ψ) due to the presence of EDL is related to electric charge density (ρ_e) by the Poisson equation [20]

$$\frac{\partial^2 \psi}{\partial x^2} + \frac{\partial^2 \psi}{\partial y^2} = -\frac{\rho_e}{\varepsilon} = -\frac{e(n^+ z^+ + n^- z^-)}{\varepsilon} \tag{9}$$

where e is the electron charge, z is the valence, n is the ion density (concentration). For a symmetric, dilute, and univalent electrolyte ($z^+=-z^-=z$), the charge density can be expressed as [21]

$$\rho_e = -2ezn_0 \sinh\left(\frac{ez\psi}{k_B T}\right) \tag{10}$$

where k_B is the Boltzmann constant, T is the absolute temperature, and n_0 is the ion concentration at the bulk region.

The scalar transport (concentration) equation for the mixing fluids can be given as

$$\frac{\partial C}{\partial t} + u\frac{\partial C}{\partial x} + v\frac{\partial C}{\partial y} = D\left(\frac{\partial^2 C}{\partial x^2} + \frac{\partial^2 C}{\partial y^2}\right) \tag{11}$$

where C is the concentration of species (sample or buffer) and D is the mass diffusion coefficient of the species.

The aforementioned mathematical model is based on a number of assumptions and approximations. First, fluids (both sample and buffer) are incompressible and Newtonian. Fluid properties, such as viscosity, permittivity, and electric conductivity, are independent of local and overall electric field strength. Moreover, ion convection effects are negligible; thus, the Poisson-Boltzmann equation is valid. Second, there is no gravitational effect, and no chemical reaction between species is considered. Third, temperature variation due to Joule heating is negligible. This can be justified for low electric field (<500 V/cm) cases investigated here. Fourth, species concentrations remain unaffected by the electromigration.

In this study, we have considered a two-dimensional (2D) (spatial) model to quantify the mixing efficiency in the microchannel. It is assumed that the variation of dependent variables in channel height direction is negligible. Note that the 2D assumption is commonly adopted in modeling of electroosmotic flow [22,23]. Patankar and Hu [24] verified the validity of this assumption in electroosmotic flow by comparing two- and three-dimensional

models. Moreover, Lin et al. [25] have shown that 2D numerical model can effectively predict the electrokinetic mixing phenomena observed (experimentally) in microchannels. However, the 3D effect might be present in the hybrid micromixer due to the presence of serpentine structures.

4 Numerical Model

The electrokinetic velocity field and concentration distribution in the micromixer can be obtained by solving Eqs. (5)–(11) with appropriate boundary conditions. However, the direct solution of the coupled system will be extremely expensive (computationally) due to different length scales associated with microfluidic devices. Generally, microfluidic channels are $1-10$ μm thick, $10-500$ μm wide, and $1-5$ cm long. In addition to the diverse spatial length scales, the EDL thickness ranges between 0.1 nm and 10 nm. The complete numerical solution of electrokinetic flows were presented in [24] based on the Debye-Huckel approximation. Later, Dutta et al. presented the steady electroosmotic flow in 2D planar geometries using spectral element method [26]. In that study, they have resolved the EDL for dilute electrolytes where the channel height was two orders of magnitude higher than Debye length (λ). However, in most microfluidic devices, the ratio of channel height to Debye length ranges between 10^3 and 10^5. Therefore, device level simulation will be computationally expensive, if one would like to resolve all length scales appropriately. The computational effort of electrokinetic flow can be minimized considerably by introducing an effective slip velocity at the channel wall [21]. This slip velocity captures the thin EDL effects on the fluid flow. This concept has been reported recently in a number of numerical works to study electrokinetic flow injection [22], electrokinetic flow control [27], etc. Thus, in this study the flow field is obtained from the continuity and Navier-Stokes equations under effective slip velocity conditions without considering the body force terms ($\rho_e\vec{E}$).

4.1 Boundary Conditions. The external electric potential distribution (ϕ) is obtained from Eq. (8), which is subjected to insulating boundary conditions ($\nabla\phi.\vec{n}=0$) on the channel surfaces. The insulating boundary condition at the channel wall is justified for the microfluidic chip because silicon, glass, poly-di-methyl siloxane (PDMS), or other insulating material is used as channel wall. The electric potentials at the inlet reservoirs are obtained from Eqs. (1)–(4), while the exit reservoir is connected to a ground ($\phi=0$). In our numerical formulation, the time-dependent boundary conditions provide unsteady electric field at every time step.

For electrokinetic relay actuation, the velocity at the slip plane is specified as

$$\vec{V}=\left(-\frac{\varepsilon\zeta}{\mu}\frac{\partial\phi}{\partial l},0\right) \tag{12}$$

where l is the direction tangent to the channel wall and ζ is the zeta potential. For simplicity, ζ is assumed constant along the channel wall. The velocities at the exit reservoir are set as fully developed ($\partial u/\partial x=0$ and $\partial v/\partial x=0$). In solving velocity field, pressure is maintained atmospheric at both inlet and exit reservoirs. That means fluid flow is entirely driven by the electrokinetic effects. Hence, the mixing performances presented in this study are for different electric potentials. Finally, to solve Eq. (11), the dimensionless species concentration is set at 0 and 1 for inlets 1 and 2, respectively, while the outlet condition is $\partial C/\partial x=0$.

4.2 Numerical Scheme and Accuracy. An h/p-type spectral element method is used to calculate electric potential (ϕ), velocity fields ($\vec{V}$), and species concentration (C) in the micromixer. The numerical algorithm employs modal spectral expansion of Jacobi polynomials in quadrilateral and unstructured triangular meshes [28]. Thus, we can discretize the complex engineering geometry with great flexibility due to the unstructured grid and can still maintain the high-order numerical accuracy. Time integration is performed by a second-order accurate, stiffly stable integration scheme. Details of the numerical scheme and convergence results were presented in [26,29,30], and hence, those will not be repeated here.

In the numerical simulation of 50 μm wide micromixer, 250 elements (50 elements in the streamwise direction and 5 elements in the cross-stream direction) are used in the active part of the mixer. This corresponds to $\Delta x=20$ μm and $\Delta y=10$ μm for h-type discretization. For 100 μm and 300 μm wide channel, the number of h-type elements in the cross-stream direction is increased to 10 and 30, respectively. By keeping the elemental discretization (h-type) of the domain fixed, the p-type refinement is employed by increasing the expansion order of polynomial within each element. One of the main features of this algorithm is the exponential decay of discretization errors on p-type refinement for a sufficiently smooth problem. Since we do not have analytical expressions for velocity and concentration fields presented in this study, p-type refinement is used to obtain grid-independent results. For electrokinetic relay mixing, the time accuracy is also very important for the simulation results. The h/p-type spectral algorithm also reduces the dispersion errors for long-time integration of transient problems [28]. In a previous study, it has been reported that this algorithm is second-order accurate in time for reciprocating flow forced convection [29]. For our numerical work, the grid-independent results are obtained at modal expansion order $N=9$ for $\Delta t=10^{-4}$ s.

5 Results and Discussion

In this section, we present the mixing performances of an electrokinetic relay micromixer without and with serpentine channel structures. Parameters considered in this numerical work are channel width, applied electric field, and relay frequency. Numerical results are obtained based on a 2D model where the variation in the height direction is neglected. The ionic concentration considered in this study is in the range between 10 mM and 100 mM, which corresponds to Debye length of 3 nm and 1 nm, respectively. Therefore, the slip (velocity) boundary condition is justified for high ionic concentration solution. Properties of water ($\rho=1000$ kg/m^3 and $\mu=0.001$ Kg/m s) are used for momentum equations as the thermodynamic properties of sample and buffer used in various bioanalytical processes are very similar to water. The simulation results presented here are performed for $\zeta=-60$ mV. This value was chosen based on experimental results in poly-di-methyl siloxane (PDMS) microchannel. Experimental results show that the zeta potential of PDMS microchannel varies between -25 mV and -80 mV, depending on the charge state and ionic concentration of buffer solution [31]. In this numerical study, species are considered to be electrically neutral. Hence, they do not alter the electrokinetic effects within the micromixer. For the concentration equation, $D=10^{-10}$ m^2/s ($\varepsilon_r=80$ and $S_c=10^4$) is used in order to obtain appropriate molecular diffusion effects in the species transport equation. In the numerical simulation, it is assumed that at $t=0$, the inlet channels 1 and 2 are filled with the buffer solution and the sample solution, respectively, while the rest of the mixing channel is filled with buffer solution.

To evaluate the mixing rate at a particular cross section, a parameter called mixing efficiency (η) is defined as the following:

$$\eta=\left(1-\frac{\int_{-W/2}^{W/2}|C-C_\infty|dy}{\int_{-W/2}^{W/2}|C_0-C_\infty|dy}\right)\times 100\% \tag{13}$$

where C is the concentration distribution in the lateral direction, C_∞ is the concentration at the ideal (complete) mixing at outlet

(which is 0.5 for our case), and C_0 is the concentration at the inlets for completely unmixed buffer or sample (0 or 1).

5.1 Effects of Channel Width. In this section, numerical simulations are performed to study whether the channel width has an effect on the mixing efficiency. Three micromixers of various channel widths (50 μm, 100 μm, and 300 μm) are considered. The applied potentials are fixed as $\phi_s=20$ V and $\phi_a=20$ V. To study the channel width effect, three relay frequencies, $f=0$ Hz, $f=5$ Hz, and $f=10$ Hz, are used. Figures 2(*a*), 2(*b*), and 2(*c*) show the numerical solution of the mixing efficiencies at the outlet ($x=1000$ μm) when channel width is 50 μm, 100 μm, and 300 μm, respectively. For no actuation case ($f=0$ Hz), the electrical potential at both inlets is 40 V. In this case, the mixing efficiency at the channel outlet is 39.2% when the channel width is 50 μm, while this value reduces to 19.6% and 6.6%, respectively, for channel widths of 100 μm and 300 μm. Although the application of an electroosmotic relay loading ($f=5$ Hz) helps improve mixing efficiency for all three micromixers, the mixing efficiency of the 50 μm wide channel is still higher than those of $W=100$ μm and 300 μm. Similar mixing tendency is observed for the 10 Hz relay frequency. Note that the mixing efficiency curves at $f=5$ Hz are oscillatory because the alternative loading of two fluids formed banded structures. However, for 10 Hz relay frequency, the mixing becomes stable at the outlet for all three channel widths considered here. The data show that a micromixer with a smaller channel width has a higher mixing efficiency than that of a larger channel width. This is because one fluid can be impinged into and mixed with the other fluid more efficiently when the channel width becomes smaller. This can be seen from the concentration contour of three micromixers shown in Fig. 3, when the mixing reached stable state at the outlet. Figures 3(*b*) and 3(*c*) show the contour plots of the three micromixers at $f=5$ Hz and 10 Hz, respectively. The blue color (dark gray) represents the concentration of buffer solution, and the pink color (light gray) represents the concentration of the sample solution. For comparison, the concentration contour of no-relay case ($f=0$ Hz) is also presented in Fig. 3(*a*). In this case, the micromixing is completely dependent on diffusion. The mixing efficiency in the 300 μm wide micromixer is the lowest among three because the diffusion length is longer than the other two micromixers.

The above numerical results imply that the maximum efficiency will be obtained if we design a micromixer with a smaller channel width. However, a decrease in channel width will impact the mixing capacity of the micromixer (flow rate of the micromixer). For the three micromixers studied here, assuming the electric field is kept the same, numerical results show that the outlet velocity (and, hence, the volume flow rate) of the micromixer is reduced 84% as the channel width is decreased from 300 μm to 50 μm. The channel width will also cause the shift of the optimal relay frequency, a frequency at which the maximum mixing efficiency occurs. As shown in Fig. 2, the maximum mixing efficiencies occurs at $f=10$ Hz for $W=50$ μm, and 100 μm, while for $W=300$ μm, the maximum mixing efficiency takes place at around $f=5$ Hz. Therefore, the numerical results suggest that a large channel width shifts the optimum relay frequency to a lower value at which fluids can be mixed more effectively. This effect will be discussed in more detail in Sec. 5.2.

5.2 Effects of Relay Frequency. In electrokinetic mixing, alternating electrokinetic sample loading facilitates larger interfacial surface areas between two fluids by stretching/folding streamlines and forming cellular structures of alternating fluids. Hence, the relay frequency is one critical factor affecting the mixing. Seven different relay frequencies are considered to optimize the mixing performance in a 50 μm wide electrokinetic micromixer. The applied potentials are fixed as $\phi_s=20$ V and $\phi_a=20$ V for $f>0$ Hz, while electric potential is 40 V at both inlets for $f=0$ Hz. The mixing efficiencies at channel outlet ($x=1000$ μm) predicted by the numerical scheme are presented in Fig. 4(*a*). For no actuation case ($f=0$ Hz), where both fluids are loaded simultaneously, the mixing efficiency is only 39.2%. Numerical results

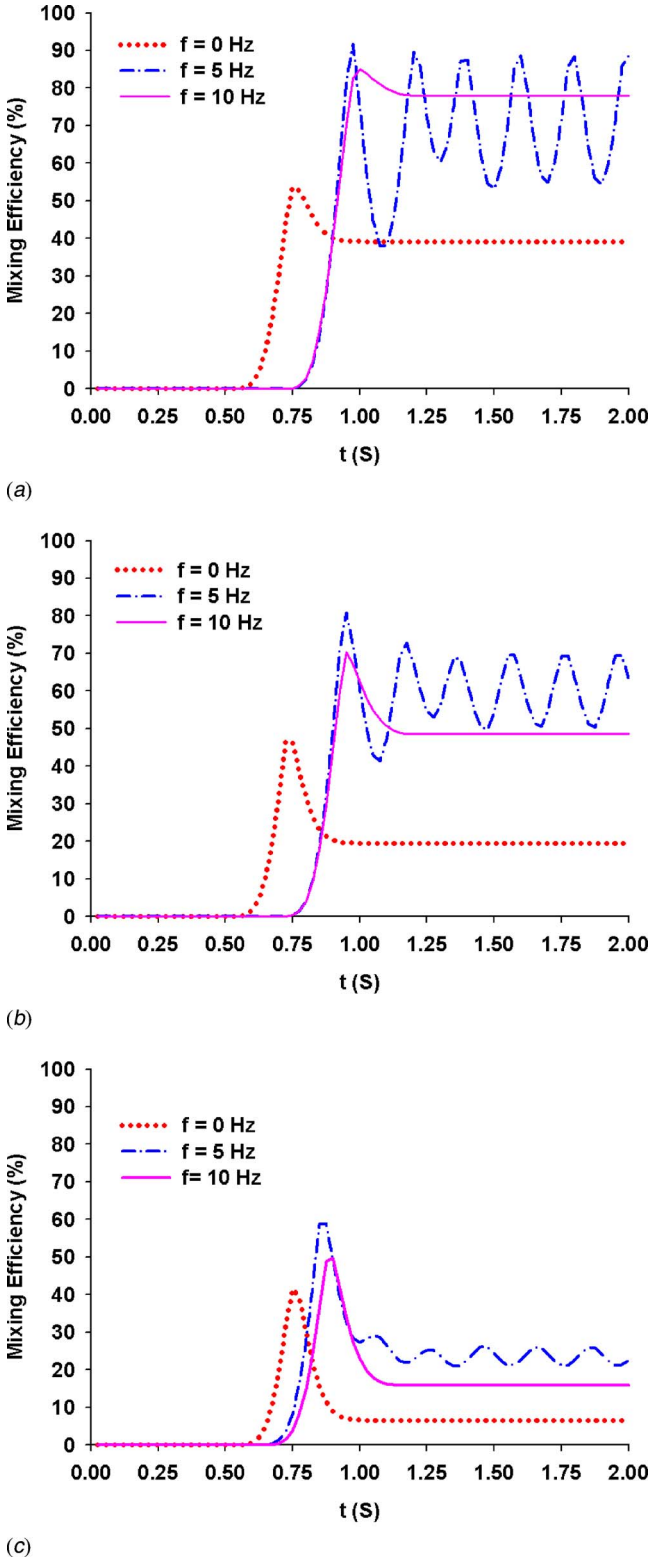

Fig. 2 Effects of microchannel width on mixing efficiency at the micromixer outlet ($x=1000$ μm) under different relay frequencies for $\phi_a=20$ V and $\phi_s=20$ V: Case (*a*) Pe=510, $W=50$ μm; (*b*) Pe=1028, $W=100$ μm; and (*c*) Pe=3208, $W=300$ μm

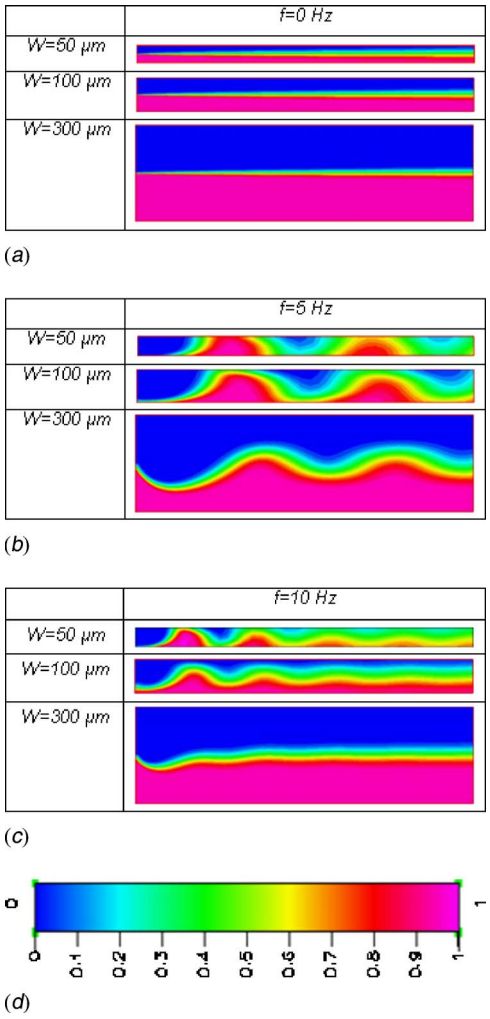

Fig. 3 Concentration contour for three electrokinetic micromixers presented in Fig. 2, under three relay frequencies (*a*) *f* =0 Hz (*b*) *f*=5 Hz, and (*c*) *f*=10 Hz. Mixing performances are presented 2 s after the initiation of electric field.

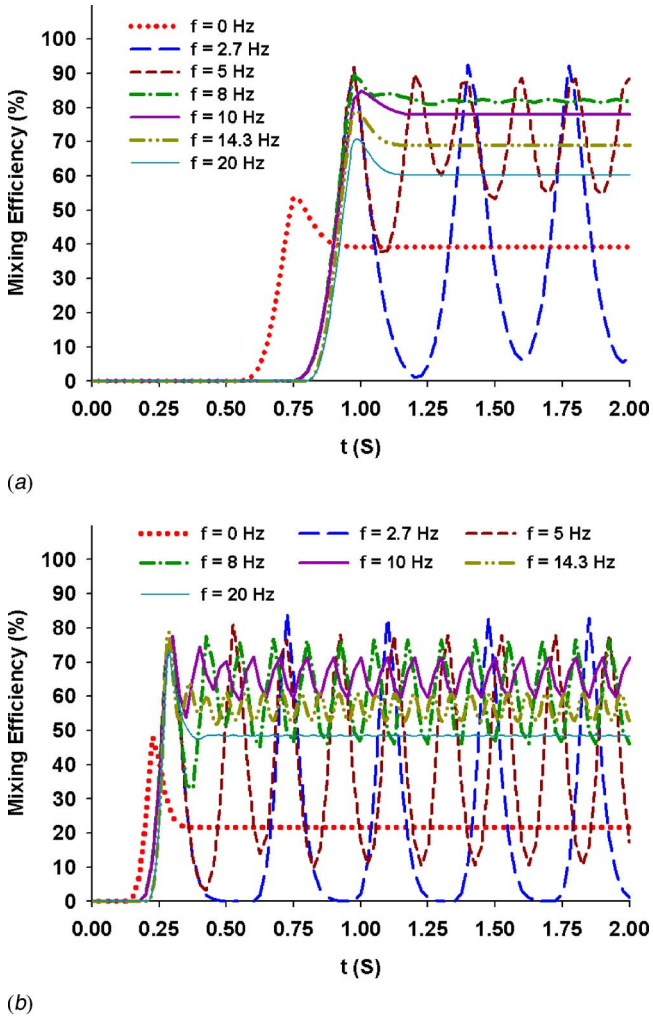

Fig. 4 Mixing efficiency for electrokinetic relay micromixer (*a*) at the micromixer outlet (x=1000 μm); (*b*) at an intermediate location (x=300 μm) under different relay frequencies. Here, ϕ_s=20 V, ϕ_a=20 V, and Pe=510.

also show that at low relay frequencies (f=2.7 Hz), the mixing efficiency is quite oscillatory, ranging from 6.1% to 92.3%. This is because at a low relay frequency, the channel width is primarily flooded by one fluid before the electrical signal is switched to the other fluid. Thus, a wide-banded composition structure is created and the mixing frequency curve has a zigzag shape, implying a uniform mixing cannot be achieved within limited time and length. These findings are consistent with results of Tang et al. [27], which predicted similar banded structures at low relay frequencies.

Thus to reach efficient mixing, the electrical potential has to be switched at a higher frequency to avoid formation of banded structure. At f=5 Hz, the mixing efficiency oscillates between 53.1% and 88.7% indicating the mixing is not yet stable. Figure 4(*a*) shows that at a relay frequency of f=8 Hz and 10 Hz, the mixing efficiency reaches 82.0% and 78.1%, respectively, and the mixing becomes stable. However, if the relay frequency is too high, one fluid cannot be impinged into the other fluid within a very short time period before the potential (voltage) signal is switched. This explains why a very high frequency ($f \geq 14.3$ Hz) is not as efficient as f=8 Hz. Figure 4(*b*) illustrates the above phenomenon at location x=300 μm. The oscillation of mixing efficiency is obvious at low frequencies, i.e., f=2.7 Hz and f =5 Hz since the banded structures have been formed. It is worth mentioning that in the absence of an electrokinetic relay mechanism (f=0 Hz), the mixing efficiency at x=300 μm is only 21.7%.

Assuming the goal of the device is to obtain maximum mixing of sample and buffer solutions, an appropriate relay frequency (the optimum relay frequency) would be necessary to increase the interfacial areas of two fluids without forming cellular structures. There are two factors that affect the maximum frequency: the impingement velocity and the channel width. The former is determined by the applied electrical field. Since the impingement velocity cannot be obtained directly, the average channel outlet velocity (U) is normally used to get an approximate optimum relay frequency f_m as [27]

$$f_m = \frac{U}{W/\sin\theta} = \frac{U\sin\theta}{W} \tag{14}$$

where θ is the Y-channel angle, and ($W/\sin\theta$) represents the travel length of impingement flow across the channel. Tang et al. pointed out that when actual relay frequency is much less than f_m ($f < 0.1 f_m$ for a case of θ=90 deg), the cellular structures are formed in the microchannel [27]. In order to remove the cellular structures, the relay frequency should be increased close to f_m.

The average mixing efficiency at the outlet of micromixers for

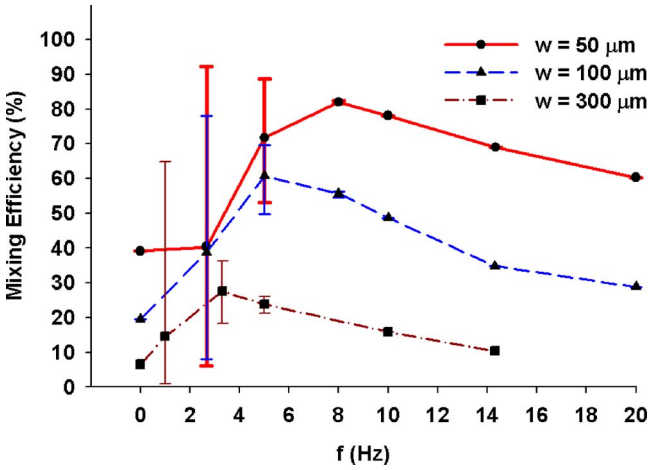

Fig. 5 Average mixing efficiency at the micromixer outlet for different electroosmotic relay frequency. Here ϕ_s=20 V and ϕ_a=20 V. The error bars indicate the oscillation range of the mixing efficiency. The data points on the curves are the average values calculated by integrating mixing efficiency over a relay cycle. The optimum frequency for 50 μm, 100 μm, and 300 μm wide micromixers are 8 Hz, 5 Hz, and 3.3 Hz, respectively.

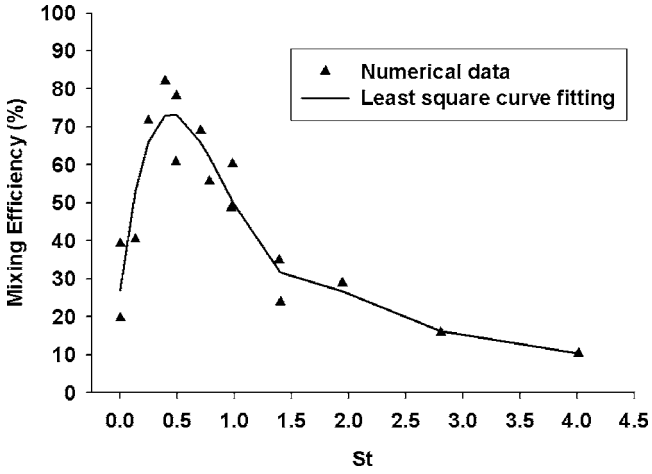

Fig. 6 Mixing efficiency variation with Strouhal number (St). For the current micromixer (θ=30 deg), the optimum efficiency takes place at St≈0.5.

different electroosmotic relay frequency is presented in Fig. 5. Numerical results of optimal relay frequency appear consistent with Eq. (14). Note that the optimum relay frequency is defined as the frequency for which the average mixing efficiency is the maximum. The average mixing efficiency is calculated by integrating mixing efficiency over a relay cycle, i.e., $\bar{\eta}=\int_1^{t_1+T}\eta(t)dt/T$, where $T=1/f$, t_1 is an arbitrary moment after a repeatable fluid pattern is reached. The error bars in Fig. 5 indicate the oscillation range of the mixing efficiency. The optimum relay frequency provided by the numerical scheme for the cases of W=50 μm and W=100 μm, as shown in Fig. 5, is 8 Hz and 5 Hz, while Eq. (14) suggests 10.2 Hz and 5.2 Hz. For W=300 μm, the numerically predicted optimum relay frequencies (~3.3 Hz) appears to have a slightly larger derivation from the prediction by Eq. (14). It is obvious that the increase of channel width reduces the mixing efficiency and shifts the optimal relay frequency to low level. It can be also predicted from Eq. (14) that the application of a lower electrical field will shift the optimal frequency to low level because it reduces the impingement velocity. Figure 6 shows the mixing efficiency dependence on Strouhal number (St=Wf/U =$(f/f_m)\sin\theta$) in electrokinetic relay mixing without any serpentine structure. The solid line is based on a fifth-order polynomial curve fit of the numerical data points. It is obvious that the maximum mixing efficiency occurs at St=sin $\theta\approx$0.5. We should note here that Eq. (14) only provides a rough prediction of optimum frequency for electrokinetic relay micromixers without passive structures. It cannot be applied to a micromixer with complicated geometries because of the complex flow patterns inside the channel, which prevents the formation of cellular structures. The channel geometry might affect the electric field, the impingement flow velocity, and travel length, and hence, the optimum frequency. Further study needs to be done to provide a more accurate formula of the optimal frequency by considering the above issues.

5.3 Effects of External Electrical Potential. Here, both fluids are driven by the electrokinetic body forces, and no external pressure head is applied in this micromixer. In the electrokinetic micromixer, the effect of externally applied electric potentials is very significant because external electric fields determine the amount of liquid pumped through particular flow geometry. To investigate the effects of externally applied electric potential, we have varied the value of both steady (ϕ_s) and fluctuating (ϕ_a) parts for a 50 μm wide electrokinetic micromixer. Figures 7(a) and 7(b) show the mixing performance at different electric field strengths at x=1000 μm and x=300 μm, respectively. In order to obtain the optimum mixing performance, effects of electrokinetic relay frequencies are also presented in Fig. 7. For a particular electrokinetic relay frequency, electric field cases with no steady component (ϕ_s=0) generates a slightly higher mixing efficiency. This is because part of the flow from one inlet channel (Y-branch) enters into the other inlet channel (Y-branch) due to potential difference, and this facilitates mixing even in the branch channels. In other words, in the absence of a steady potential component, two fluids started interacting with each other in the branch channels. However, the early mixing created in the branch channels slows down the fluid entering the mixing channel. As a result, it requires more mixing time to reach a stable mix than that of the other case presented here. In both figures, mixing efficiency curve at f =0 Hz (ϕ_1=40 V and ϕ_2=40 V) is included. It is obvious that electroosmotic relay driving with appropriate relay frequency (f ≈10 Hz, St=0.49) enhances micromixing. Note that the electrical potential will also affect the optimum rely frequency in terms of affecting the fluid velocity in the microchannel.

5.4 Hybrid Micromixing Schemes. Although electrokinetic micromixer has demonstrated mixing ability with self-sustained pumping, the overall mixing efficiency is relatively low (<80%) for the case presented in this study. There are several factors contributing to this low mixing performance. First, while the electrokinetic relay mechanism stretches the fluid streams to increase the interfacial surface area, its influence is limited in the contact regions of two fluids near the entrance. Second, at the downstream of the micromixer, because the velocity in the y direction is negligible, chaotic advection that distorts and elongates fluid interface is missing. Third, without chaotic advection, mass diffusion is restrained due to limited interfacial area between two fluids. One way to induce advection is to introduce "complicated" structures in the mixing channel.

In order to reach a high mixing efficiency (>95%), asymmetric serpentine structures are introduced in the mixing chamber as shown in Fig. 1(b). Like the electrokinetic micromixer, the main driving mechanism is alternating electrokinetic forces. This particular design is introduced to bring in chaotic advection and force the fluid to change its directions dramatically to induce efficient mixing. Note that the entry region of the micromixer is adopted to keep the flow rate of two inlets approximately the same. The numerical results of concentration distributions in hybrid micromixer are presented in Fig. 8(a) for an electrokinetic relay fre-

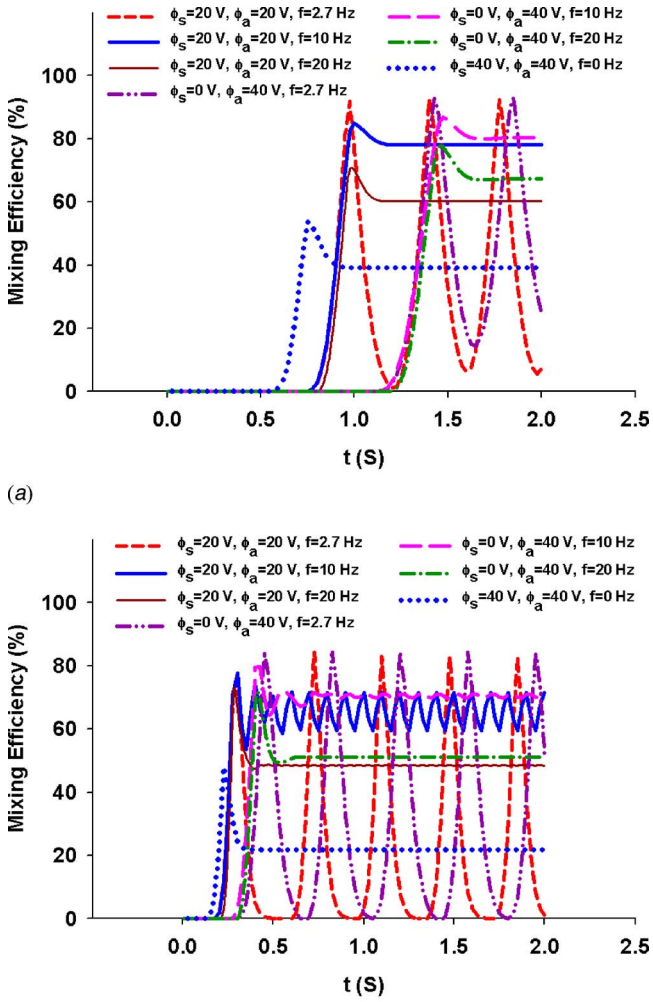

Fig. 7 Effects of applied electric potential on mixing efficiency (*a*) at the micromixer outlet (x=1000 μm) and (*b*) at an intermediate location (x=300 μm) under different relay frequencies. Here, Pe=510.

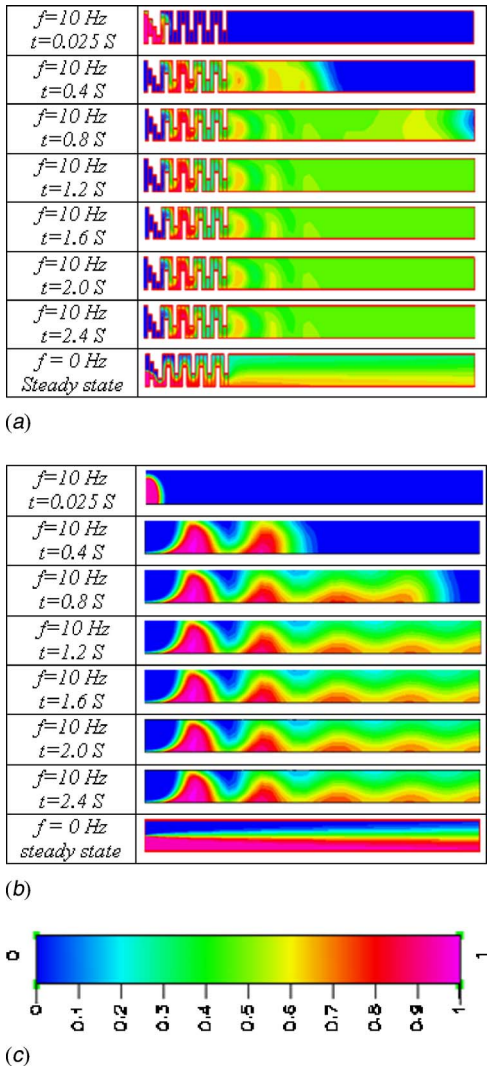

Fig. 8 Concentration contour for (*a*) the hybrid micromixer and (*b*) the electrokinetic micromixer at different times. The corresponding micromixer design is presented in Figs. 1(*b*) and 1(*a*), respectively. Here, ϕ_s=20 V, ϕ_a=20 V, and Pe=262 and 510 for the electrokinetic and hybrid micromixers, respectively.

quency of 10 Hz. Here the dimensions of the channels are W =50 μm, L_x=200 μm, L=1000 μm, θ=30 deg, and W_a =12.5 μm. The alternating component of electric potential is set at 20 V and the steady component of electric potential is fixed at 20 V. The blue color (dark gray) represents the concentration of buffer solution and the pink color (light gray) represents the concentration of the sample solution. Like previous cases, at time t =0, inlet channels 1 and 2 are filled with the buffer (blue) and the sample (pink) fluids, respectively (not shown in Fig. 8), while the rest of the mixing chamber contains buffer. To compare the mixing process, the concentration contour for electrokinetic relay micromixer without asymmetric serpentine structures is also presented (Fig. 8(*b*)) for the same frequency (f=10 Hz).

In the electrokinetic relay micromixer, mixing starts happening at $t>0$ due to selective pumping of sample and buffer. As shown in Fig. 8(*b*), starting at t=0.4 s, stable mixing is achieved in the middle of the channel, and the mixed fluid starts to fill in the downstream section. The mixing condition in the absence of relay frequency is also presented in the last row in Fig. 8(*b*). It is obvious that in the absence of electrokinetic relay loading, the mixing is dominated by the diffusion and the mixing performance is low. On the other hand, in the hybrid micromixer (see Fig. 8(*a*)), a complete mixing can be achieved rapidly due to the presence of asymmetric serpentine structures. In the hybrid micromixer, the flow begins to mix at t=0.025 s. At t=0.4 s, the mixing front enters the straight part of the micromixer and efficient mixing is developed (Fig. 8(*a*)). At t=0.8 s, the microflow is already highly mixed at x=300 μm. The average mixing efficiency reaches 84.9% at this position. At x=500 μm, this number becomes 95.6%. Starting from t=0.8 s, the highly mixed flow begins to fill in the rest of the channel. Eventually, a completely mixed flow is developed in the downstream and the mixing efficiency reaches 98.6% at the channel outlet. However, in the absence of electroosmotic relay driving, a relatively low mixing efficiency of 82.0% is obtained. The mixing performances at x=1000 μm and at x =300 μm are presented in Figs. 9(*a*) and 9(*b*), respectively. These results indicate that the hybrid micromixing scheme, which utilizes electroosmotic relay driving and asymmetric serpentine structures, offers a highly efficient and stable mixing within a very short time.

6 Summary and Conclusions

Effective mixing of liquids is essential in many applications, such as drug delivery, DNA analysis/sequencing, pheromone syn-

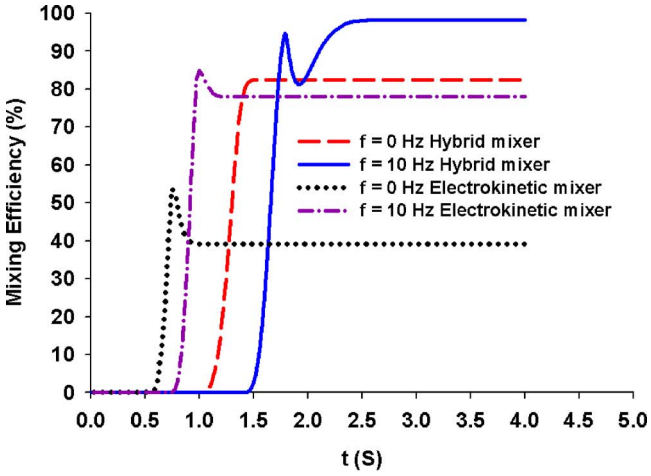

(*a*)

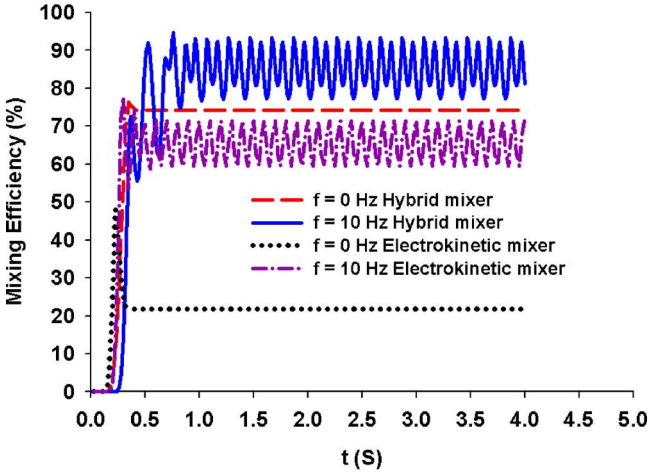

(*b*)

Fig. 9 Comparison of mixing efficiency (*a*) at the micromixer outlet (x=1000 μm) and (*b*) at an intermediate location (x =300 μm) with and without asymmetric serpentine structures. Here, ϕ_s=20 V and ϕ_a=20 V. The Peclet numbers for the electrokinetic and hybrid micromixers are 510 and 262, respectively.

thesis in microbioreactors, and biological/chemical agent detections. Rapid mixing can reduce the analysis time and permit high throughput in lab-on-a-chip devices. For rapid mixing of liquids, a Y-form hybrid electrokinetic-passive micromixer is presented.

The effects of various design parameters, such as channel width, relay frequency, external electric potential, and asymmetric serpentine structures, have been studied. In an electrokinetic micromixer, the critical (optimum) relay frequency depends on the channel width and the applied electric potential. For a wider microchannel, the maximum efficiency is obtained at relatively low actuation frequency, while the optimum relay frequency obtained from numerical prediction is relatively high for a narrower channel. Moreover, for a particular relay frequency, the mixing performance is better if the channel width becomes smaller. Simulation results also show that the mixing performance is slightly better if the steady component of electric potential is zero. In this case, the mixing originates at the branch channel. However, this case takes longer to reach a stable mixing state.

Numerical results also illustrate that pure electrokinetic relay actuation is not enough for a complete micromixing within a short distance and time. In a hybrid micromixer, the asymmetric serpentine structure plays an active role in ultrafast mixing within a short distance. With this hybrid micromixer, a very high mixing efficiency (95.6%) can be reached within 1.0 s at x=500 μm for a 50 μm wide channel. However, passive serpentine structures induce flow impedance and reduces the flow velocity in the micromixer. For the same applied potentials, the flow velocity in the hybrid micromixer is only 51% of that of an electrokinetic micromixer.

Acknowledgment

This work was supported by the Washington Technology Center and University of Akron Firestone Research Initiative Fellowship.

Nomenclature

C = dimensionless concentration
D = mass diffusivity, m^2/s
e = electron charge, C
$\vec{E}$ = electric field, V/m
f = relay frequency, Hz
k_B = Boltzmann constant, J/K
l = direction tangent to the channel wall
L = length of the mixing chamber, μm
L_x = length of the inlet channel, μm
m = alternating parameter
n^+/n^- = ion density of positive or negative charges
P = pressure, N/m^2
Pe = Peclet number, UW/D
Re = Reynolds number, UW/v
Sc = Schmidt number, v/D
St = Strouhal number, fW/U
t = time, s
T = temperature, K
u = streamwise velocity, μm/s
U = streamwise velocity at channel outlet, μm/s
v = cross-stream velocity, μm/s
W = width of the microchannel, μm
W_a = width of asymmetric structures, μm
x = x position of the coordinate system, μm
y = y position of the coordinate system, μm
z^+/z^- = valence of positive or negative charges

Greek Letters

ε = permittivity, F/m
ε_r = relative permittivity
ϕ = external electric potential, V
ϕ_1 = electric potential at inlet 1, V
ϕ_2 = electric potential at inlet 2, V
η = mixing efficiency
μ = dynamic viscosity, kg/m s
λ = Debye length, nm
θ = angle of Y-channel, degree
ρ_e = electric charge density, C/m^3
ρ_f = density of the fluid, kg/m^3
σ = electrical conductivity, $1/\Omega$ m
ψ = electrokinetic potential, V
ζ = zeta potential, mV

Subscripts

a = alternating component
e = electric
f = fluid
o = bulk region or inlets
s = steady component
∞ = complete mixing state

References

[1] Bessoth, F. G., DeMello, A. J., and Manz, A., 1999, "Microstructure for Efficient Continuous Flow Mixing," Anal. Commun., **36**, pp. 213–215.

[2] Losey, M. W., Jackman, R. J., Firebaugh, S. L., Schmidt, M. A., and Jensen, K. F., 2002, "Design and Fabrication of Microfluidic Devices for Multiphase Mixing and Reaction," J. Microelectromech. Syst., **11**, pp. 709–717.
[3] Hong, C. C., Choi, J. W., and Ahn, C. H., 2004, "A Novel In-Plane Passive Microfluidic Mixer With Modified Tesla Structures," Lab Chip, **4**, pp. 109–113.
[4] Mengeaud, V., Josserand, J., and Girault, H. H., 2002, "Mixing Processes in a Zigzag Microchannel: Finite Element Simulations and Optical Study," Anal. Chem., **74**, pp. 4279–4286.
[5] Liu, R. H., Stremler, M. A., Sharp, K. V., Olsen, M. G., Santiago, J. G., Adrian, R. J., Aref, H., and Beebe, D. J., 2000, "Passive Mixing in a Three-Dimensional Serpentine Microchannel," J. Microelectromech. Syst., **9**, pp. 190–197.
[6] Park, S. J., Kim, J. K., Park, J., Chung, S., Chung, C., and Chang, J. K., 2004, "Rapid Three-Dimensional Passive Rotation Micromixer Using the Breakup Process," J. Micromech. Microeng., **14**, pp. 6–14.
[7] Stroock, A. D., Dertinger, S. K. W., Ajdari, A., Mezic, I., Stone, H. A., and Whitesides, G. M., 2002, "Chaotic Mixer for Microchannels," Science, **295**, pp. 647–651.
[8] Jacobson, S. C., McKnight, T. E., and Ramsey, J. M., 1999, "Microfluidic Devices for Electrokinetically Driven Parallel and Serial Mixing," Anal. Chem., **71**, pp. 4455–4459.
[9] Oddy, M. H., Santiago, J. G., and Mikkelsen, J. C., 2001, "Electrokinetic Instability Micromixing," Anal. Chem., **73**, pp. 5822–5832.
[10] Yang, Z., Matsumoto, S., Goto, H., Matsumoto, M., and Maeda, R., 2001, "Ultrasonic Micromixer for Microfluidic Systems," Sens. Actuators, A, **93**, pp. 266–272.
[11] Lu, L. H., Ryu, K. S., and Liu, C., 2002, "A Magnetic Microstirrer and Array for Microfluidic Mixing," J. Microelectromech. Syst., **11**, pp. 462–469.
[12] Tsai, J. H., and Lin, L., 2002, "Active Microfluidic Mixer and Gas Bubble Filter Driven by Thermal Bubble Micropump," Sens. Actuators, A, **97–98**, pp. 665–671.
[13] Rong, R., Choi, J. W., and Ahn, C. H., 2003, "A Functional Magnetic Bead/Biocell Sorter Using Fully Integrated Magnetic Micro/Nano Tips," *Proc. IEEE MEMS*, IEEE, New York, pp. 530–533.
[14] Suzuki, H., and Ho, C. M., 2002, "A Magnetic Force Driven Chaotic Micro-Mixer," *Proc. of 15th IEEE International Conference on MEMS*, IEEE, New York, pp. 40–43.
[15] Deval, J., Tabeling, P., and Ho, C. M., 2002, "A Dielectro-phoretic Chaotic Mixer," *Proc. of 15th IEEE International Conference on MEMS*, IEEE, New York, pp. 36–39.
[16] Liu, R. H., Yang, J., Pindera, M. Z., Athavale, M., and Grodzinski, P., 2002, "Bubble-Induced Acoustic Micromixing," Lab Chip, **2**, pp. 151–157.
[17] Bottausci, F., Mezic, I., Meinhart, C. D., and Cardonne, C., 2004, "Mixing in the Shear Superposition Micromixer: Three-Dimensional Analysis," Philos. Trans. R. Soc. London, Ser. A, **362**, pp. 1001–1018.
[18] He, B., Burke, B. J., Zhang, X., Zhang, R., and Regnier, F. E., 2001, "A Picoliter-Volume Mixer for Microfluidic Analytical Systems," Anal. Chem., **73**, pp. 1942–1947.
[19] Johnson, T. J., Ross, D., and Locascio, L. E., 2002, "Rapid Microfluidic Mixing," Anal. Chem., **74**, pp. 45–51.
[20] Probstein, R. F., 1994, *Physicochemical Hydrodynamics*, Wiley, New York.
[21] Dutta, P., and Beskok, A., 2001, "Analytical Solution of Combined Electroosmotic/Pressure Driven Flows in Two-Dimensional Straight Channels: Finite Debye Layer Effects," Anal. Chem., **73**, pp. 1979–1986.
[22] Ren, L., Sinton, D., and Li, D., 2003, "Numerical Simulation of Microfluidic Injection Processes in Crossing Microchannels," J. Micromech. Microeng., **13**, pp. 739–747.
[23] Ermakov, S. V., Jacobson, S. C., and Ramsey, J. M., 2000, "Computer Simulation of Electrokinetic Injection Techniques in Microfluidic Devices," Anal. Chem., **72**, pp. 3512–3517.
[24] Patankar, N. A., and Hu, H. H., 1998, "Numerical Simulation of Electroosmotic Flow," Anal. Chem., **70**, pp. 1870–1881.
[25] Lin, C. H., Fu, L. M., and Chien, Y. S., 2004, "Microfluidic T-Form Mixer Utilizing Switching Electroosmotic Flow," Anal. Chem., **76**, pp. 5265–5272.
[26] Dutta, P., Beskok, A., and Warburton, T. C., 2002, "Numerical Simulation of Mixed Electroosmotic/Pressure Driven Flows," Numer. Heat Transfer, Part A, **41** pp. 131–148.
[27] Tang, Z., Hong, S., Djukic, D., Modi, V., West, A. C., Yardley, J., and Osgood, R. M., 2002, "Electrokinetic Flow Control For Composition Modulation in a Microchannel," J. Micromech. Microeng., **12**, pp. 870–877.
[28] Karniadakis, G. E., and Sherwin, S. J., 1999, *Spectral HP Element Methods for CFD*, Oxford University Press, London.
[29] Sert, C., and Beskok, A., 2003, "Numerical Simulation of Reciprocating Flow Forced Convection in Two-Dimensional Channels," ASME J. Heat Transfer, **125**, pp. 403–412.
[30] Dutta, P., Beskok, A., and Warburton, T. C., 2002, "Electroosmotic Flow Control in Complex Microgeometries," J. Microelectromech. Syst., **11** pp. 36–44.
[31] Keisuke, H., and Dutta, P., 2005, "Flow Diagnosis in a Trapezoidal Microchannel," *Proc. of JSME conference on Fluid Mechanics*, JSME, Paper No. AM05-07-002.